J Radioanal Nucl Chem (2015) 304:563–570
DOI 10.1007/s10967-014-3857-8

Extracted species of Np(IV) complex with diglycolamide functionalized task specific ionic liquid: diffusion, kinetics and thermodynamics by cyclic voltammetry

Arijit Sengupta · M. S. Murali · P. K. Mohapatra · M. Iqbal · J. Huskens · W. Verboom

Received: 16 July 2014 / Published online: 20 December 2014

Abstract This paper reports a first-ever cyclic voltammetric study and the electrochemical characterization of Np(IV) complexes with task-specific ionic liquid with appended diglycolamide (DGA-TSIL) ligand dissolved in the room-temperature ionic liquid 1-butyl-3-methylimidazolium bis(trifluoromethylsulfonyl)imide (C_4mimNTf_2). The results are compared with molecular entity, *N*,*N*,*N*′,*N*′-tetraoctyl diglycolamide (TODGA) dissolved in the same diluent. The diffusion coefficient (D) values were determined using the Randles–Ševcik equation. The standard rate constant (k_s) values were also computed for the Np(IV)/Np(III) electrode redox reaction. The activation energy for diffusion (E_a) and thermodynamic parameters for the redox reactions of the Np complexes were determined and compared.

Keywords Task specific ionic liquid · Neptunium · Cyclic voltammetry · Diffusion coefficient · Thermodynamic parameters

List of symbols

ν	Scan rate, potential sweep rate
$E_p^c, E_{P1/2}^c$	Cathodic peak potential, half-wave cathodic peak potential respectively
E_p^a	Anodic peak potential
GC	Glassy carbon
D_0 or D	Diffusion coefficient
$(i_p^c)_{diff}$	Diffusion controlled cathodic peak current
n	Number of electrons involved in the electrode reaction
F	Faraday constant
A	Area of electrode
C_0	Concentration of the analyte in the solution/bulk
α	Charge transfer coefficient
n_α	Number of electrons in the rate-determining step
T	Absolute temperature in Kelvin
R	Ideal gas constant
A_o	Pre-exponential factor
E_a	Energy of activation for diffusion
D_{ox}, D_{red}	Diffusion coefficients of oxidized and reduced species respectively
γ_{ox}, γ_{red}	Activity coefficients of oxidized and reduced species respectively
$\Delta G°$, $\Delta H°$ $\Delta S°$	Changes in standard Gibbs free energy, enthalpy and entropy respectively
$E^o_{ox/red}$	Standara potential

A. Sengupta · M. S. Murali (✉) · P. K. Mohapatra
Radiochemistry Division, Bhabha Atomic Research Centre, Mumbai 400085, India
e-mail: muralimurali63@rediffmail.com

M. Iqbal · J. Huskens · W. Verboom
Laboratory of Molecular Nanofabrication, MESA+ Institute for Nanotechnology, University of Twente, P.O. Box 217, 7500 AE Enschede, The Netherlands

Introduction

Increase in energy demand coupled with depleted fossil fuel and environmental issues, makes nuclear energy the most-probable alternative source of energy. Further, development of fast neutron reactors ensure the much higher burn up of the fuel as well as mitigate the problem of long-lived minor actinides by burning them to shorter-lived fission products [1]. ^{237}Np is one of the important long-lived minor actinides (MA), which have long term

environmental concerns for safe geologic disposal. The fate of these MA, in the event of their release to the geosphere and migration to the environment, depends on their oxidation state, solubility of complexes and complexing ability with various ligands employed for their separation. As for ^{237}Np, its separation and quantitative determination from high-level waste solutions (HLW) originating from nuclear fuel reprocessing by aqueous route is one of the challenging aspects for the separation chemists aiming for actinide-partitioning by solvent extraction [2]. Its complex chemistry, due to its variable oxidation states makes its study more difficult, but nevertheless required. As is practised all over the world, the aqueous route for nuclear fuel reprocessing plutonium uranium extraction process (PUREX) is beset with problems such as secondary waste generation, radiation damage to the solvent etc. It is seen that the above process, while focussing on only plutonium and uranium, leaves neptunium in different streams of feed, organic extract, raffinate etc. without its clear separation to any one stream. Alternate fuel reprocessing systems such as pyrochemical processing are advantageous in that they are compact and separations are achievable by electrochemical means. While mostly mixtures of fused salts are the basis of pyrochemical reprocessing of (molten salt) reactor fuels, room temperature ionic liquids (RTILs) also form potential media for this purpose. Applications of RTILs as alternative diluent media are numerous in many fields now [3–7]. Although they were projected as green solvents, their toxicity, environmental impact are less known and need more studies. However, one of the foremost research areas for possible application of these neoteric solvents is in nuclear fuel reprocessing and waste management. RTILs are generally defined as ionic liquids composed of organic cations and organic or inorganic anions and melt at temperatures below 100 °C. The more frequently investigated RTILs consist of organic cations such as 1,3-dialkylimidazolium, quaternary ammonium, *N*-alkylpyridinium, *N,N′*-dialkylpyrrolidinium, and alkylphosphonium and organic or inorganic anions, especially halides, hexafluorophosphate (PF_6^-) and bis(trifluoromethylsulfonyl) imide, ($N(SO_2CF_3)_2^-$) or NTf_2. RTILs are shown to have a number of attractive properties, such as thermal stability, nonflammability, low or negligible vapor pressure, and wide electrochemical potential windows. The application of ionic-liquid-based solvent systems for actinide extraction has been recently reviewed [8–11]. With the synthesis of task-specific ionic liquids (TSILs), appended with ligating groups analogous to relevant organic extractants, the field of applications is becoming richer as recently demonstrated in literature [12–19]. TSILs (functionalized ionic liquids) have many advantages over solvent systems that contain an extractant dissolved in a RTIL. TSILs are often found to remain exclusively in the RTIL phase under all process conditions, in addition to giving selectivity for a metal ion. Of the various TSILs that have been tested for actinide-ion extraction, diglycolamide- (DGA) -based TSILs have recently been studied and compared with their analogous solvent systems containing the molecular DGA extractants in conventional RTILs for the extraction of actinides, etc. from nitric acid and simulated high-level waste (HLW) solutions originating from nuclear fuel reprocessing [20, 21]. RTILs, often display a variety of extraction mechanisms depending on several parameters such as the nature of cation or anion constituting the ionic liquid, substituents present on cation, aqueous phase acidity etc. [4, 9]. Hence, there is a need of fundamental studies on RTILs or TSILs to unravel their chemical/electrochemical aspects for interpreting the effects on the separation-chemistry of actinides, lanthanides, and important fission product elements.

In order to understand the redox chemistry of these actinides in solutions, especially of RTILs, and to apply them for nuclear related tasks stated above, electrochemical investigations are very useful. The electrochemical aspects of RTILs are reviewed in literature [8, 22]. Also, there are a few reports on the electrochemistry of Np in its various oxidation states, especially in acidic aqueous and ionic liquid solutions [23–27]. However, to the best of our knowledge, an electrochemical study on the complexes of Np(IV) with the above task-specific ionic liquid is not reported previously.

As a part of our ongoing studies, electrochemical aspects on f-elements dissolved in RTILs are published previously [28–30]. The present paper deals with a cyclic voltammetry study of Np(IV) and its complex with a TSIL based on diglycolamide (DGA-TSIL) and compared with that based on the molecular entity, namely, tetraoctyldiglycolamide (TODGA) dissolved in the RTIL 1-butyl-3-methyl-imidazolium bis(trifluoromethylsulfonyl) imide (C_4mimNTf_2).

Experimental

Materials

N,N,N′,N′-tetra-*n*-octyldiglycolamide (TODGA, >97 %) was obtained from Thermax Ltd, India, and was characterized by various physicochemical methods, as reported previously [28]. The detailed synthesis and characterization of DGA-TSIL is given elsewhere [30].The structures of both ligands used in the present study are given in Fig. 1. The diluent C_4mimNTf_2 was procured from IoliTec, Germany at >99 % purity [31]. All other reagents were of AR grade. The actinide tracer (^{237}Np) was used from laboratory stock and its purity was checked by alpha-spectrometry.

Fig. 1 Structures of the ligands used

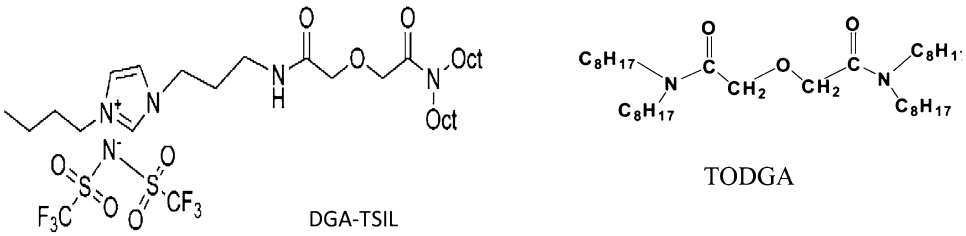

Preparation of Np(IV) complexes in room temperature ionic liquids

Solutions of Np (0.04 mM) were prepared in the +4 oxidation state by the addition of appropriate reducing agents (ferrous sulphamate followed by hydroxylamine hydrochloride) in a 3.0 M nitric acid solution. Then the aqueous phase was equilibrated with an equal volume of organic phase containing 100 mM TODGA or DGA-TSIL in C_4-mimNTf$_2$ for 3 h to achieve maximum extraction of the Np(IV) complexes into the ionic liquid phase. This time was found to be sufficient to attain equilibrium. The organic phases were separated after centrifuging and subsequently appropriately diluted to make 3.5 mL solutions to be taken into an electrochemical cell for cyclic voltammetric studies.

Instrumentation

Cyclic voltammograms of the solutions were recorded using an Autolab -PGSTAT-030 (Metrohm, Switzerland) equipped with an IF 030 interface. It has facilities for data handling, supported by the GPES software. A three-electrode system comprising platinum wires as working, pseudo-reference, and counter electrodes was used.

Cyclic voltammetric studies

A small glass cylindrical cell of 2.5 cm diameter and ~7 mL capacity was used with a Teflon cap containing inlets to insert the reference electrode, working electrode, and counter electrode. 3.5 mL solutions of different Np(IV) complexes prepared above in C_4mimNTf$_2$ were taken in the cell separately. The cell was flushed with argon for 15 min. This cell was placed in a jacketed two-layer glass container maintained at constant temperature with a circulatory water-bath (Lauda, Germany) with a precision of 0.1 °C. The cyclic voltammograms for the oxidized forms of the metal ion complexes and for pure C_4mimNTf$_2$ were recorded with linear sweep potential settings starting from a positive potential (1.25 V) to a negative potential (−2.0 V) and reversing it back to the starting voltage. For Np in 3 M nitric acid, this was from 1.6 to −0.25 V at different scan rates (0.01–3 V/s in most cases) at temperatures varying from 298 to 328 K. IR compensation was applied during the studies.

Results and discussion

Cyclic voltammetry of Np in aqueous HNO_3 and organic complexes of Np(IV) in RTIL

Figure 2 gives the cyclic voltammograms (CV) for the extracted complexes of Np(IV) with the ligands TODGA and DGA-TSIL in C_4mimNTf$_2$ along with that for Np in nitric acid and a CV for neat C_4mimNTf$_2$ (without Np) at a scan rate of 0.1 V/s at 25 °C. The CV of Np in nitric acid was referred to the CV prior to the adjustment of the oxidation state of Np to (IV). So, all the redox peaks of Np in different oxidation states were expected in it. Therefore, within the relatively small potential window in 1 M HNO_3 (−0.2 to +1.5 V), with characteristic peaks for the redox species of Np were as given below. E_p^c(VI/V) = 1.16 V; E_p^a(V/VI) = 1.27 V; E_p^c(IV/III) = −0.15; E_p^a(III/IV) = −0.05. These peak positions are similar to those obtained in literature [27]. That these peaks are not due to the reduction of nitric acid is corroborated by Kim et al. [32], where they had shown that below 2 M nitric acid no

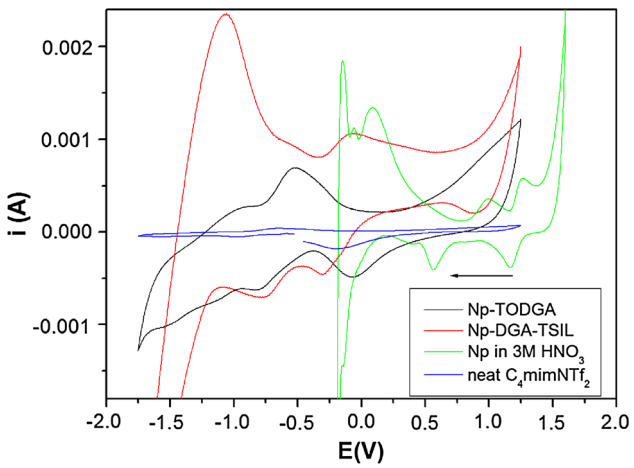

Fig. 2 CV of Np(IV) in nitric acid and extracted complex of Np(IV) by TODGA and DGA-TSIL in RTIL C_4mimNTf$_2$, scan rate 0.1 V/s, T = 25 °C

reduction peak was observed at GC electrode. The remaining peaks might be due either to other oxidation states of Np or to nitric acid. The potential window in the case of the RTIL is larger than that of nitric acid. The CVs of the Np(IV) complex with DGA-TSIL and TODGA (Fig. 2), show a reduction peak resulting from the diluent C_4mimNTf$_2$. Also, the amount of nitric acid extracted into the RTIL by the ligands was expected to be low since the basicities were not too high. Hence, the peaks arising out of extracted nitric acid were too faint to characterize. The peak positions due to the redox reactions of the Np(IV)-complexes in both systems are given in Table 1. Since these positions were obtained after the oxidation state of Np was adjusted to IV and its extraction into the respective RTIL phases, the peaks indicate oxidation state transitions of Np from IV to III and III to IV. Since there are only a few, e.g. [23] previous references for the peak positions of Np in a RTIL, direct comparisons could not be made due to the nature of ionic liquid used in [23] was a mixture of $AlCl_3$ and 1-*n*-butyl pyridinium chloride without any complexing ligand—a situation different from the present one. The oxidation potentials (Np(III)/(IV)) are negative for the DGA-TSIL and TODGA complexes. The order of the reduction potentials (Np(IV)/(III)) was found to be TODGA > DGA-TSIL (more negative to less negative). This shows that Np(IV) is most resistant to reduction in TODGA or in other words, the Np(IV) complex with TODGA is more stable than that with DGA-TSIL. If the distribution coefficient of Np (defined as the ratio of activity of Np(IV) extracted to the organic phase to that remained in the aqueous phase, i.e. $Np(IV)_{org}/Np(IV)_{aq}$ where the subscripts org and aq represent the organic phase and aqueous phase respectively) is a measure of the stability of the extracted complex. For Np(IV) complexation, distribution coefficient values of 17.6 and 0.35 were obtained for TODGA and DGA-TSIL, respectively [30], supporting the stability order given above. Table 2 summarizes the the peak potentials at different temperatures for both Np-TODGA and Np-DGA-TSIL systems at a constant scan rate.

Table 1 Anodic and cathodic peak positions for the Np(IV) complexes with the different ligands at a scan rate of 0.1 V/s, 318 K

System	E_p^c, V (Np(IV/III))	E_p^a, V (Np(III/IV))	$E_0' = (E_p^a + E_p^c)/2$, V	$Np(IV)_{org}/Np(IV)_{aq}$
Aqueous HNO_3	−0.14	0.086		
0.01 M TODGA in C_4mimNTf$_2$	−0.8	−0.55	−0.675	4.4 (17.6)[#]
0.04 M DGA-TSIL in C_4mimNTf$_2$	−0.91	−0.003	−0.47	0.35

[#] Estimated value in parenthesis is for 0.04 M TODGA, stoichiometry remaining same at 1:1

Determination of diffusion coefficients of the Np(IV) complexes

Figure 3 presents the CVs of the metal ion complexes with the ligands as a function of the scan rate. The cathodic and anodic peak potentials show a marginal shift with scan rates of 0.01–3.0 V/s. The fact that the peak shifts at low scan rates of 0.025–0.15 V/s (e.g. in the cathodic peak potentials) indicates that the redox processes of these metal ions are quasi-reversible or involving irreversible charge transfer for the reduction of them. Thus, assuming that these processes in the RTIL are controlled by both diffusion and charge transfer kinetics, the appropriate relationship between the cathodic diffusion peak current [$(i_p^c)_{diff}$] and the scan rate (ν) for a soluble–soluble irreversible/quasi-reversible system is given by Eq. (1) below [28, 33].

$$\left(i_p^c\right)_{diff} = 0.496\, nFAC_0\sqrt{D_0(\alpha n_\alpha F\nu/RT)}^{1/2}, \quad (1)$$

where A is the electrode area in cm^2 (= 1.68 cm^2), C_0 is the concentration of the corresponding metal ion in mol/cm^3, D_0 is the diffusion coefficient in cm^2/s, F is the Faraday constant, 'n' is the number of exchanged electrons (1 for the Np(IV/III) couple), v is the potential sweep rate in V/s, α is the charge transfer coefficient, n_α is the number of electrons transferred in the rate-determining step, and T is the absolute temperature in K. A plot of (i_p^c) versus $v^{1/2}$ should give a straight line if the electrochemical reaction as supposed above is true. The linear relationship in all the cases clearly follows from Fig. 4. The slopes of the straight lines give a value of $0.496\ nFAC_0\sqrt{D_0}\ (\alpha n_\alpha\ F/RT)^{1/2}$. Herein, the only unknown product αn_α, obtainable from the Eq. (2) below, [33] when substituted in the value of the slope, gives the diffusion coefficient D_0.

$$E_p^c - E_{p1/2}^c = 1.857\, RT/\alpha n_\alpha F \quad (2)$$

Table 2 Peak potentials of Np^{4+} complexes at different temperature obtained from cyclic voltammograms at scan rate 0.1 Vs^{-1}

System	Temp (K)	E_p^c (V)	E_p^a (V)	E^0 (V)	$E_p - E_p^{1/2}$ (V)
Np^{4+}-TODGA	298	−0.51	−1.07	−0.79	−0.082
	308	−0.52	−0.94	−0.73	−0.079
	318	−0.55	−0.8	−0.67	−0.069
	328	−0.59	−0.43	−0.51	−0.068
Np^{4+}-DGA-TSIL	298	−1.25	−0.8	−1.02	−0.007
	308	−1.22	−0.38	−0.81	−0.01
	318	−0.91	−0.003	−0.45	−0.06
	328	−0.8	0.12	−0.34	−0.16

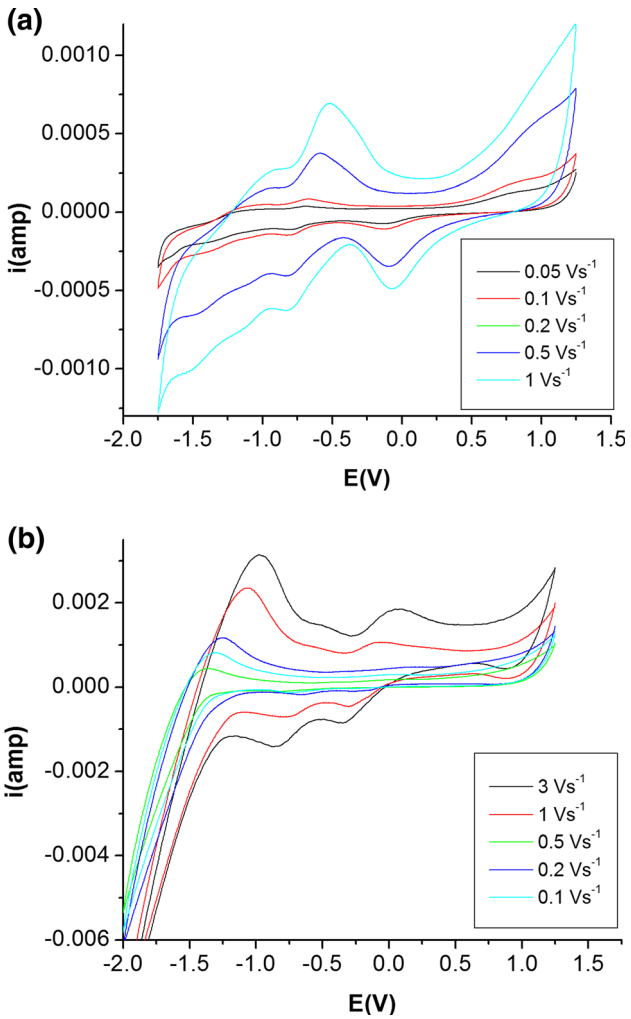

Fig. 3 CV of Np(IV) complexes with **a** TODGA and **b** DGA-TSIL in C_4mimNTf$_2$, at different scan rates at 308 K

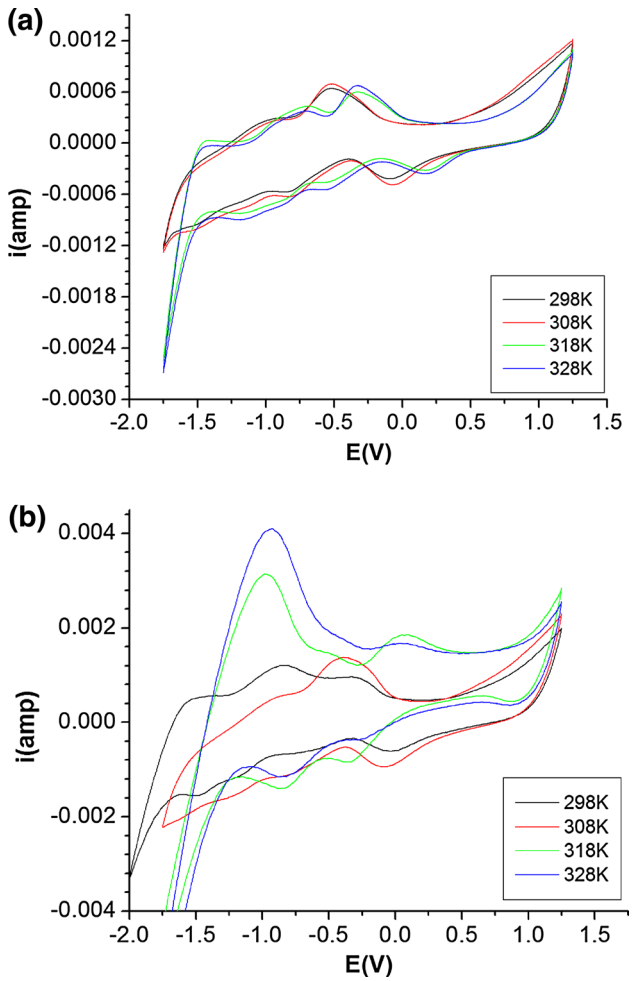

Fig. 4 CV of Np(IV) complexes with **a** TODGA and **b** DGA-TSIL in C_4mimNTf$_2$, at different temperatures at a scan rate 0.1 V/s

Here, the E_p^c and $E_{p1/2}^c$ represent the cathodic peak potential and cathodic peak potential when the current is half of its peak value. These values were determined at a particular scan rate using the in-built software which has provision to manually select the baseline and peak-find search functions (Table 2). The D_0 values computed from the slopes at different temperatures (the CVs for the Np complexes with ligands TODGA and DGA-TSIL at different temperatures at a fixed scan rate are given in Fig. 5) are summarized in Table 3. From Table 3 it is clear that with increasing temperature the diffusion coefficient also increased, which can be attributed either to a decrease in the viscosity of the medium or a decrease in the size (bulkiness) of the complexes or both. The order of the diffusion coefficients of the Np(IV) complexes associated with possible cluster formation or aggregation from solvation at 298 K was found to be TODGA > DGA-TSIL and at other temperatures it was in reverse order (Table 3). The increase in D_0 for the Np(IV) complex with a particular ligand with temperature may be due to a decrease of the viscosity.

Determination of the activation energy E_a

The activation energy for the diffusion of the metal ion can be related to the diffusion coefficient through the Arrhenius equation (Eq. 3) [33].

$$D_0 = A_0 \exp(-E_a/RT), \quad (3)$$

where A_o is the pre-exponential factor and E_a is the corresponding activation energy. Therefore, a plot of ln D_0 versus $1/T$ gives a straight line as shown in Fig. 6 (left) with a slope of $(-E_a/R)$. The activation energy values for the diffusion of Np(IV) complex are listed in Table 3.

Estimation of thermodynamic parameters

The tetravalent neptunium complexes with the ligands in C_4mimNTf$_2$ undergo reduction to Np(III) according to the following equation.

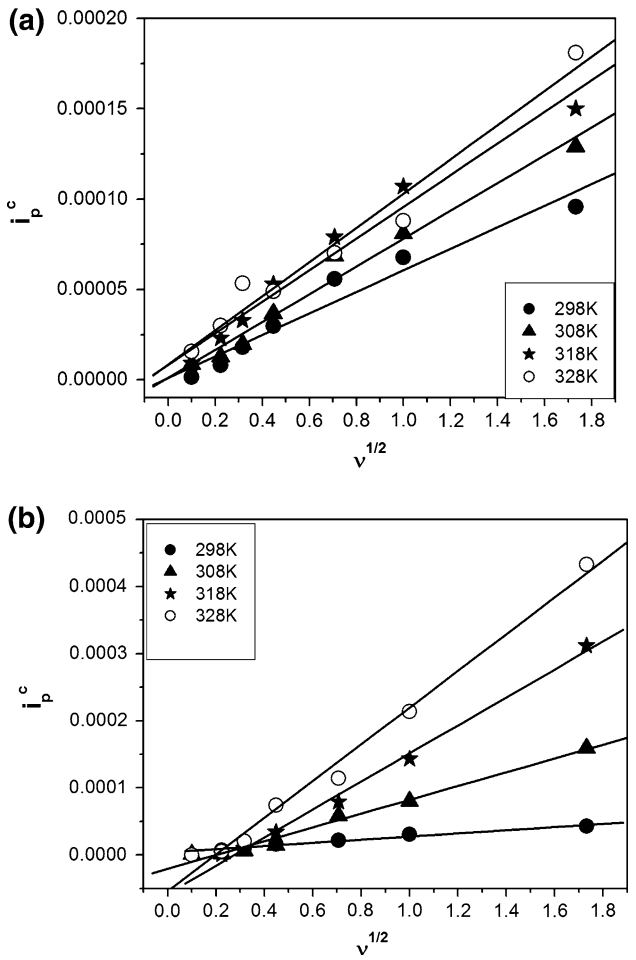

Fig. 5 i_c^p versus $v^{1/2}$ at different temperatures for NP(IV) complexes with **a** TODGA and **b** DGA-TSIL in C_4mimNTf$_2$, scan rate = 0.1 V/s

Table 3 Diffusion coefficients calculated using Eq. (2) from the slopes of the plots of Fig. 5, and energy of activation for diffusion for the Np(IV) complexes with the different ligands

System	Temp (K)	D_0 (cm^2/s)	E_a (kJ/mol)
Np(IV)-TODGA complex	298	1.25E−015	24.8 ± 0.4
	308	2.09E−015	
	318	2.70E−015	
	328	3.16E−015	
Np(IV)-DGA-TSIL complex	298	7.51E−016	98.3 ± 2.1
	308	3.67E−015	
	318	1.54E−014	
	328	2.57E−014	

$$\mathrm{Np(IV)} + \mathrm{e} \leftrightarrow \mathrm{Np(III)} \tag{4}$$

Since, the cathodic and anodic peak potentials determined were against that of the pseudo reference electrode, one can, by approximation, relate these values to the "apparent" standard potential $E^{0*}_{ox/red}$ by the following equations [33]

$$E_p^c = E^{0*}_{ox/red} - 1.11\,RT/nF - RT/nF\ln(\sqrt{D_{ox}}/\sqrt{D_{red}}), \tag{5}$$

$$E_p^a = E^{0*}_{ox/red} + 1.11\,RT/nF - RT/nF\ln(\sqrt{D_{ox}}/\sqrt{D_{red}}), \tag{6}$$

where

$$E^{0*}_{ox/red} = E^{0}_{ox/red} + RT/nF\ln(\gamma_{ox}/\gamma_{red}) \tag{7}$$

Here, $E^{0*}_{ox/red}$ and γ represent the standard potential and activity coefficient, respectively and others have their usual meaning. D_{ox} and D_{red} represent the diffusion coefficients of oxidized and reduced species respectively and it was assumed here that both have the same value. The reduction reaction involved n (= 1) electron transfer. The apparent standard potentials $E^{0*}_{ox/red}$ determined using Eq. (8) are plotted against T in Fig. 6 (right) showing that $E^{0*}_{ox/red}$ increases with increasing temperature.

$$E^{0*}_{ox/red} = \left(E_p^a + E_p^c\right)/2 \tag{8}$$

from linear regression of the experimental data, from which it was deduced that the $E^{0*}_{ox/red}$ values are related to the temperature by the following expressions.

$$E^0(\mathrm{Np(IV)/(III)\text{-}TODGA}) = (-3.84) + (0.012)\,T\,V \tag{9}$$

$$E^0(\mathrm{Np(IV)/(III)\text{-}DGA\text{-}TSIL}) = (-8.36) + (0.021)\,T\,V \tag{10}$$

The standard Gibbs energy ($\Delta G°$) for the reactions can be determined using Eq. (11) with the assumption that the solution is dilute and the activity coefficients are unity.

$$\Delta G° = -nFE^{0*}_{ox/red} \tag{11}$$

The expression for $\Delta G°$ as a function of temperature can be derived from the above E^0 for the redox reactions given as

$$\Delta G°(\mathrm{Np\text{-}TODGA}) = (-370.56) + (0.96)\,T \text{ kJ/mol} \tag{12}$$

$$\Delta G°(\mathrm{Np\text{-}DGA\text{-}TSIL}) = (-806.74) + (1.93)\,T \text{ kJ/mol} \tag{13}$$

Comparing Eqs. (12), (13) with the Gibbs–Helmholtz Eq. (14), the changes in enthalpy ($\Delta H°$), entropy ($\Delta S°$), and Gibbs energy ($\Delta G°$) for the above reactions were calculated.

$$\Delta G° = \Delta H° - T\Delta S° \tag{14}$$

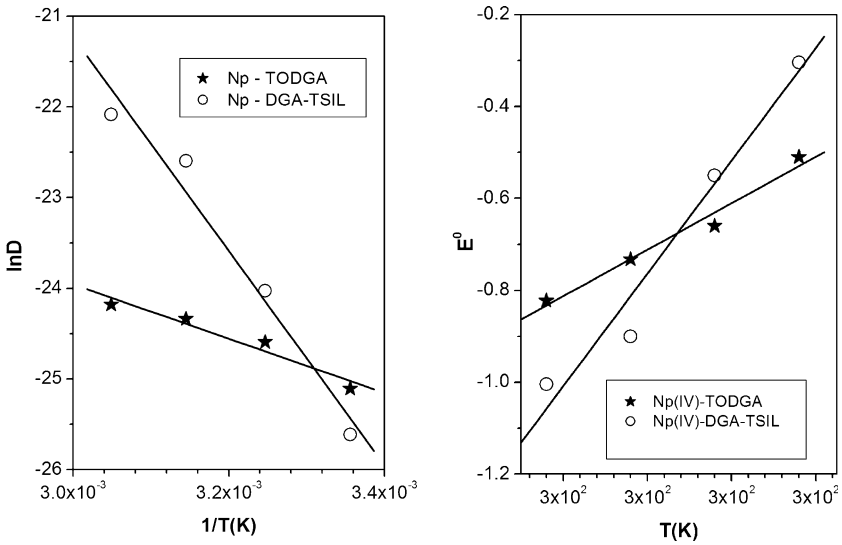

Fig. 6 ln D versus $1/T$ (*left*) and E^0 versus T (*right*) for Np(IV) complexes extracted by DGA-TSIL and TODGA in $C_4mimNTf_2$

From the above equations it can be deduced, that for the redox couples involving complexes of Np(IV) with TODGA and DGA-TSIL, the $\Delta H°$ values are negative, thereby showing that the reactions are exothermic and enthalpy driven. On the other hand, the $\Delta S°$ values are low positive.

Calculation of the rate constant k_s

Since the scan rate variation underlined the fact that apart from diffusion, electron exchange might also be a slow process, the rate constant for the heterogeneous reaction was determined by the following equation [33, 34].

$$k_s = 2.18[D_0(\alpha n_\alpha)\, v\, F/RT]^{1/2} \exp\left[\alpha^2 nF\left(E_c^p - E_a^p\right)/RT\right] \text{ cm/s}, \quad (15)$$

where the terms have their usual meaning. The electrode reaction can be classified [34] as reversible when $k_s \geq 0.3\ v^{1/2}$ cm/s, quasi-reversible when $0.3\ v^{1/2} \geq k_s \geq 2.0 \times 10^{-5}\ v^{1/2}$ cm/s, and irreversible when $k_s \leq 2.0 \times 10^{-5}\ v^{1/2}$ cm/s. Based on the values obtained (see Table 3), the redox reactions of Np were classified mostly as quasi—reversible except in the case of Np-DGA-TSIL complex where the redox reaction was found to be irreversible at 298 K. It can also be seen from Table 4 that the rate constant values were found to be of same order of those listed in Ref. [23] for Np(IV/III) in basic melts of room temperature ionic liquids at 40 °C.

Conclusions

Cyclic voltammetry of the Np-complexes with the ligands TODGA and DGA-TSIL in $C_4mimNTf_2$ was carried out. The diffusion coefficients of the complexes and the standard rate constants for the mono-electron exchange reactions were determined. The activation energy values were deduced using the Arrhenius equation and thermodynamic parameters were derived using linear regression of the data. The redox reactions of the Np complexes with both ligands were exothermic. The changes in the entropy values were not significant underlining that the reorganization of the complex during the redox reaction does not take place to alter the number of entities significantly.

Table 4 Nature of the electrochemical reaction based on k_s for the Np complexes with the different ligands, $v = 0.1$ V/s at different temperatures

System	T (K)	K_s (cm/s)
Np(IV)-TODGA	298	1.08E−03
	308	1.38E−03
	318	6.95E−03
	328	1.29E−02
Np(IV)-DGA-TSIL	298	1.09E−05
	308	7.70E−05
	318	1.92E−04
	328	2.38E−04

Acknowledgments The authors wish to acknowledge Dr. A. Goswami, Head, Radiochemistry Division, BARC, for his constant support and encouragement.

References

1. http://www.world-nuclear.org/info/Current-and-Future-Generation/
2. Murali MS, Bhattacharayya A, Raut DR, Kar AS, Tomar BS, Manchanda VK (2012) J Radioanal Nucl Chem 294:149–153
3. Huddleston JG, Willauer HD, Swatloski RP, Visser AN, Rogers RD (1998) Chem Commun 44:1765–1766

4. Blanchard LA, Hancut D, Beckman EJ, Brennecke JF (1999) Nature 399:28–29
5. Fadeev AG, Meagher MM (2001) Chem Commun 44:295–296
6. Cocalia VA, Jensen MP, Holbrey JD, Spear SK, Stepinski DC, Rogers RD (2005) Dalton Trans 15:1966–1971
7. Visser AE, Rogers RD (2003) J Solid State Chem 171:109–113
8. Venkatesan KA, Srinivasan TG, Rao PRV (2009) J Nucl Radiochem Sci 10:R1–R6
9. Sun X, Luo H, Dai S (2012) Chem Rev 112:2100–2128
10. Kolarik Z (2013) Solvent Extr Ion Exch 31:24–60
11. Vasudeva Rao PR, Venkatesan KA, Rout A, Srinivasan TG, Nagarajan K (2012) Sep Sci Technol 47:204–222
12. Li N, Fang G, Liu B, Zhang J, Zhao L, Wang S (2010) Anal Sci 26:455–459
13. Loe-Mie F, Marchand G, Berthier J, Sarrut N, Pucheault M, Blanchard-Desce M, Vinet F, Vaultier M (2010) Angew Chem 122:434–437
14. Visser AE, Swatloski RP, Reichert WM, Mayton R, Sheff S, Wierzbicki A, Davis JH, Rogers RD Jr (2001) Chem Commun 580:135–136
15. Harjani JR, Friscic T, MacGillivray LR, Singer RD (2008) Dalton Trans 34:4595–4601
16. Ouadi A, Klimchuk O, Gaillard C, Billard I (2007) Green Chem 9:1160–1162
17. Ouadi A, Gadenne B, Hesemann P, Moreau JJE, Billard I, Gaillard C, Mekki S, Moutiers G (2006) Chem Eur J 12:3074–3081
18. Odinets IL, Sharova EV, Artyshin OI, Lyssenko KA, Nelyubina YV, Myasoedova GV, Molochnikova NP, Zakharchenro EA (2010) Dalton Trans 39:4170–4178
19. Sengupta A, Mohapatra PK, Iqbal M, Huskens J, Verboom W (2013) Sep Purif Technol 118:264–270
20. Sengupta A, Mohapatra PK, Iqbal M, Verboom W, Huskens J (2012) Dalton Trans 41:6970–6979
21. Barrosse-Antle LE, Bond AM, Compton RG, O'Mahony AM, Rogers EI, Silvester DS (2010) Chem Asian J 5:202–230
22. Schoebrechts JP, Gilbert B (1985) Inorg Chem 24:2105–2110
23. Kim SY, Asakura T, Morita Y, Uchiyama G, Ikeda Y (2004) J Radioanal Nucl Chem 262:311–315
24. Yamamura T, Watanabe N, Yano T, Shiokawa Y (2005) J Electrochem Soc 152:A830–A836
25. Kim SY, Asakura T, Morita Y (2005) Radiochim Acta 93:767–770
26. Kitatsuji Y, Kimura T, Kihara S (2010) J Electroanal Chem 641:83–89
27. Sengupta A, Murali MS, Mohapatra PK (2013) J Radioanal Nucl Chem 298:405–412
28. Sengupta A, Murali MS, Mohapatra PK (2013) J Radioanal Nucl Chem 298:209–217
29. Sengupta A, Murali MS, Mohapatra PK (2014) J Rare Earths 32:641–647
30. Mohapatra PK, Sengupta A, Iqbal M, Huskens J, Verboom W (2013) Chem Eur J 19:3230–3238
31. Ansari SA, Mohapatra PK (2013) Radiochim Acta 101:163–168
32. Kim KW, Lee EH, Choi IK, Yoo JH, Park HS (2000) J Radioanal Nucl Chem 245:301–308
33. Rao CJ, Venkatesan KA, Nagarajan K, Srinivasan TG, Vasudeva Rao PR (2009) Electrochim Acta 54:4718–4725
34. Bard AJ, Faulkner IR (1980) Electrochemical methods fundamentals and applications. Wiley, New York